

Modeling of the Flexible Disk Grinding Process: Part I - Model Development

Song-Min Yoo
Department of Mechanical Engineering
Kyunghee University

Abstract

In this study, a new model for flexible disk grinding process will be proposed. A grinding mechanism with a grinding disk attached to the rubber platen has been introduced. Since the spinning axis is fixed and only the disk is deflected with respect to this axis, earlier model is not adequate to represent this process. A new dynamic process model includes an assumption that the disk is deflected locally around the middle of its radial span between the spinning axis and the disk tip instead of several continuous deflection points along the radial span of the disk. Detailed kinematic analysis is proposed as for the removed portion during the process. Cutting force component and depth of cut profile trend is compared with the measured result.

1 Introduction

Among manufacturing processes, a surface finishing technique plays an important part in the production process for obtaining high machining accuracy, consistent product quality and good surface roughness of the workpiece.

A lot of emphasis has been put on the grinding process due to its important role in removing discrepancies in shape and size and improving surface finish. Even though grinding is a process with a high level of quality and precision, it is one of the least understood processes. Kegg[1] emphasized the importance of developing an improved understanding of the grinding process because:

- information on grinding process performance as a function of grinding parameters is used in process planning and machine setup,
- increased productivity without deterioration in surface quality is possible,
- understanding stock removal rate as a function of the various grinding parameters involved and prediction of grinding burn is desirable and

- performance of the process changes as the wheel condition changes or wears.

Previous work has been done aimed at the above areas in the directions of grinding process performance evaluation, process monitoring with proper sensing systems and process modeling. Among them, grinding process modeling was used in an attempt to describe the grinding wheel interaction with the workpiece and to find the influence of the process parameters. These studies have been provided as an analytical tool to predict and to improve the output surface quality. A dynamic model of the flexible disk grinding process has been developed by Kurfess[2]. In this model, a grinding wheel was put in the grinder mount which was pivoted at one end and was connected by a spring at the other end to the milling machine quill. Since the whole grinder mount rotates around the pivot, the location of the grinding wheel spinning axis also varies during the process. Simplified but effective model was developed and the output surface quality was related to the location of the disk tip point[3]. Process parameters such as grinding force, power and volume (metal, stock) removal rate were simulated.

Several attempts have been tried to analyze grinding process focusing on the topography of wheel or output product. Grinding wheel profiles were obtained by using a convolution of random waves[4] and a continuous time series model[5]. König[6] used a numerical method to describe workpiece topography over a contact length with the grinding wheel. A mathematical model for the grinding forces as chip formation forces and friction forces with respect to different workpiece materials was used by Lichun[7]. An analytical belt force model was developed to investigate the force between the belt grinder and driving pulley or a workpiece[8,9]. A process simulation model using a single grit was implemented by Dornfeld[10] to observe the effect of various rake angles. The elastic deflection effect of a wheel and a workpiece because of the contact was considered for output surface generation[11,12]. Dynamic characteristics of the process have been utilized to develop a flexible disk grinding process model[2].

The Charles Stark Draper Laboratory (CSDL) has developed a force-vision controlled robotics grinding system. The applications were removal of weld bead[2], a task common to the automotive and shipbuilding industries, and the automatic grinding of cast iron stamping dies[13]. Even though several analytical models were developed, further detailed explanation is required in order to achieve closer prediction by a developed model. This study is aiming at developing another analytical model of the flexible disk grinding process using a fortified kinematical relationship.

2 Development

2.1 Previous Model

Fig. 1 shows a picture of the grinding process using flexible disk. During the process, the disk is continuously deflected due to the infeed action of the workpiece. In this study, a rubber platen to which the grinding disk was attached was used as a flexible grinder.

The inadequacy of the previous models require that an improved model be developed to better match the actual grinding process. The assumption for the disk deflection for the improved model development is that the grinding disk tip was actually deflected locally around the middle of its radial span contrary to the previous assumption that the disk is deflected with respect to the disk center. Fig. 2 shows the grinding process model. As a primary variable, df (deflection arm distance), represents the distance from the deflection point J to the disk tip B (Fig. 2).

$$v_n = v_{fx} \sin \alpha + \dot{\alpha} Rsm \quad (1)$$

$$\begin{aligned} P &= f_t v_t \\ &= w f_t R_s \\ &= w \mu f_n R_s \\ &= w \mu K_s (\alpha_0 - \alpha) \frac{R_s}{Rsm} \end{aligned} \quad (2)$$

$$area = A D \quad (3)$$

$$Z = f_n R_s = K_s (\alpha_0 - \alpha) = k_1 P - k_2 \quad (4)$$

From the above equations, characteristic equation can be summarized as:

$$\dot{\alpha} = -\frac{v_{fx} \sin \alpha}{Rsm} + \frac{1}{area Rsm} [k_1 (w \mu K_s (\alpha_0 - \alpha) \frac{R_s}{Rsm}) - k_2] \quad (5)$$

• where

- α_0 : initial disk orientation angle
- α : current disk angle
- $\dot{\alpha}$: disk rotational angular velocity
- μ : frictional coefficient between the disk and the workpiece

A : length of the disk in contact with workpiece (contact length)

B : disk tip

C : center of contact length

D : thickness of the workpiece

G : center of the disk

$area$: contact area between the disk and the workpiece

f_n : normal force component

f_t : tangential force component

k_1, k_2 : constants relating Z and P

K_s : torsional spring constant

m : moment

Z : volume (stock, metal) removal rate

P : supplied power

R_s : distance from disk center to contact area center (effective radius)

v_n : normal velocity component

v_t : tangential velocity component

v_{fx} : feed velocity

w : wheel velocity

Especially, Rsm represents the distance from the deflection center J to the contact length center C as:

$$Rsm = df - \frac{A}{2} \quad (6)$$

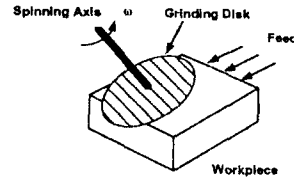


Figure 1 Flexible Disk Grinding Process

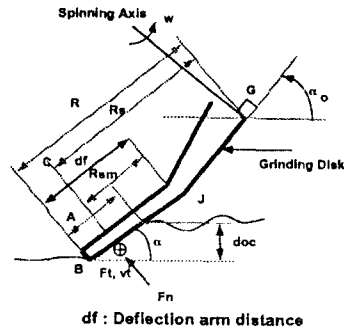


Figure 2 Previous Model

2.2 Stages of the Grinding Process

Variables such as, *area* and *Rsm* are updated from the grinding process geometry. If we consider the grinding process with rectangular workpiece *EFHI* and initial disk angle α_0 ($0^\circ < \alpha_0 < 90^\circ$) with respect to *EF*, the grinding process can be divided into 3 stages which are defined as (Fig. 3):

- Entrance stage : Transitional stage from the initial contact (*E* is on the line *BG*) between the disk and a workpiece until disk tip *B* is fully embedded in the workpiece (*B* is on the line *EI*) or from disk position 1 to disk position 2 in Fig. 3
- Between edges stage : Stage from the end of the entrance stage until the disk begins to leave the workpiece (*I* is on the line *BG*) or from disk position 2 to disk position 3 in Fig. 3
- Exit stage : Transitional stage from the end of the between edges stage until the disk leaves the workpiece (*B* is on the line *HI*) or from disk position 3 to disk position 4 in Fig. 3

The following condition is required for the existence of the between edges stage.

$$\overline{EI} > \frac{doc_{b0}}{\tan \alpha_{b0}} \quad (7)$$

- where

\overline{EI} : distance from *E* to *I*

*doc*_{b0} : depth of cut at the beginning of the between edges stage

α_{b0} : disk angle at the beginning of the between edges stage

Even though the above classification has been drawn with respect to a rectangular (flat top surface) specimen, the same rules can be applied for a specimen with an arbitrary surface profile.

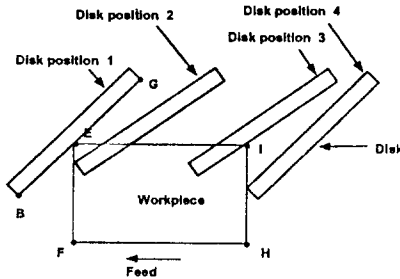


Figure 3 Grinding Process Stages

2.3 Modified Model

Previous model developed lacks explanations regarding detailed trend of contact length *A* and *area* displayed in Eq. (3). During the incremental simulation time duration, average value of the contact length *A* was used neglecting the contact surface orientation change. In other words, the portion removed by the disk would be arbitrary shape instead of trapezoid assumed previously. This study is focusing on the kinematic analysis of the removed area during entrance and between edges stages defined earlier.

2.3.1 Entrance Stage

Fig. 4 shows transient process at entrance stage during Δt . Grinding disk will move from *bg* to *de* and be deflected to *cf*. Therefore, volume removed during Δt is *bcfg*. Following relationships can be derived from the disk and workpiece geometry.

$$acf = \frac{1}{2}(A1 \cos \alpha + \Delta x)^2 \tan \alpha \quad (8)$$

$$abg = \frac{1}{2}(A1 \cos \alpha)^2 \tan \alpha \quad (9)$$

$$\begin{aligned} cdef &= \frac{1}{2}(Rsm + \frac{A2}{2})^2 \Delta \alpha - \frac{1}{2}(Rsm - \frac{A2}{2})^2 \Delta \alpha \\ &= Rsm A2 \Delta \alpha \end{aligned} \quad (10)$$

where $A2$ is $A1 + \frac{\Delta x}{\cos \alpha}$. Finally, removed volume *acfg* can be found as

$$\begin{aligned} acfg &= A1 \Delta x \sin \alpha + (\Delta x)^2 \tan \alpha + Rsm A1 \Delta \alpha \\ &\quad + \frac{Rsm \Delta x \Delta \alpha}{\cos \alpha} \end{aligned} \quad (11)$$

Since volume removal rate can be calculated by *acfg*/ Δt , characteristic equation during between edges stage is summarized as follows from Eqs. (4) and (11).

$$\dot{\alpha} = -\frac{v_f \sin \alpha}{Rsm} + \frac{1}{Rsm(A1 + \frac{\Delta x}{\cos \alpha})} (k_1 P - k_2) \quad (12)$$

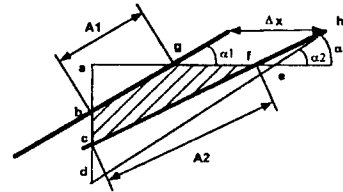


Figure 4 Entrance Stage Geometry

2.3.2 Between Edges Stage

Fig. 5 displays the removed portion of the workpiece during infinitesimal time duration Δt . A disk will proceed from *af* to *be* and be deflected to *cd* due to the inflected motion of the process. Actual removed portion is *acdf*. This can be found by subtracting *abc* and *bcde*

from $abdf$.

$$\begin{aligned} bcde &= \frac{1}{2}df^2 \Delta\alpha - \frac{1}{2}(df - A)^2 \Delta\alpha \\ &= \frac{1}{2}A(2df - A)\Delta\alpha \end{aligned} \quad (13)$$

From triangles abc and bcg with infinitesimal angle assumption of $\angle bac$ and $\angle bgc(\theta)$, $\angle bgc$ can be found to be $\frac{df \Delta\alpha}{\Delta x}$.

$$abc = \frac{1}{2}(\Delta x)^2 \theta = \frac{1}{2}df \Delta x \Delta\alpha \quad (14)$$

Since $abef$ and Δx are $Asin\alpha v_{fx} \Delta t$ and $v_{fx} \Delta t$, removed portion $acdf$ would be as follows.

$$acdf = Asin\alpha v_{fx} \Delta t + \frac{1}{2}(df \Delta x - A^2 + 2dfA)\Delta\alpha \quad (15)$$

Since volume removal rate can be calculated by $acdf/\Delta t$, characteristic equation during between edges stage is summarized as follows from Eqs. (4) and (15).

$$\dot{\alpha} = \frac{1}{A Rsm + \frac{1}{2}df \Delta x} (-A sin\alpha v_{fx} + k1 P - k2) \quad (16)$$

Characteristic representation during the exit stage will follow Eq. (5) in this study. One of the important parameters with the flexible disk grinding process model is Rsm which can be described as follows.

$$Rsm = \frac{h}{2 \sin \alpha} + \frac{1}{2 \cos \alpha} \left(\frac{h}{\tan \alpha_0} + v_{fx} t_b \right) \quad (17)$$

$$Rs = \frac{R}{2} + \frac{h}{2 \sin \alpha} \quad (18)$$

$$Rs = \frac{R}{2} + \frac{1}{2 \cos \alpha} \left(\frac{h}{\tan \alpha_{e0}} + v_{fx} t_e \right) \quad (19)$$

• where

h : distance from disk center to specimen top surface

t_b : time passed since the beginning of entrance stage

α_{e0} : angle at the beginning of the exit stage

t_e : time passed since the beginning of the exit stage

Above results are for entrance, between edges and exit stage respectively.

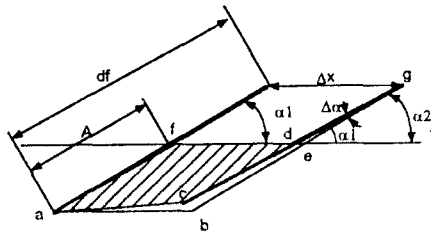


Figure 5 Between edges stage geometry

2.4 Experimental Conditions and Results

In order to check the validity of the model, a wood specimen with 2 inch (50.8 mm) width and height (\overline{EF} and \overline{EF} in Fig. 3) oak wood specimen was used. 0.5 inch (12.7 mm) thickness was employed for this specimen to eliminate the lateral dimension effect of the disk and to prevent breakage and serious lateral deflection during the process due to the tangential force component f_t . The depth of cut was 0.5 inch (12.7 mm) for this specimen. This is substantially larger than that used in practice but is suitable for model evaluation as the transition stage will be more evident.

A 3M brand 120 grain disk (type C, closed coat and aluminum oxide) was attached to a 7 inch (177.8 mm) diameter rubber platen as a grinding wheel. This wheel was attached to the milling machine spindle. The workpiece was mounted on a strain gauge dynamometer. Force signals from the strain gauge were amplified by BHL strain gauge conditioning unit. The output profile and roughness was measured by an optical scanning system[14].

As mentioned earlier, the purpose of this study is to find the improved model of the flexible disk grinding process specifying the kinematic relationship of volume removal process (geometric shape of removed volume). Fig. 6 displays the results of experimental measurement, earlier model and improved model respectively. Improved model showed better capability in predicting cutting force component while worse result was obtained with depth of cut profile trend compared to earlier model represented by Eq. (5).

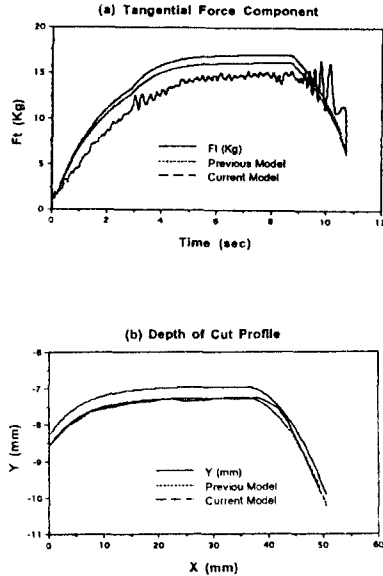


Figure 6 Ft and Depth of Cut Trend

3 Conclusions

It was observed that the Kurfess' model was not sufficient enough to represent the grinding process with flexible disk. Therefore, a modified model including the local disk deflection length, df , and three different process stages was introduced earlier. Another improved model was developed with emphasis on the following areas.

- Process dynamics from infeed motion with flexible disk
- Three process stages defined earlier
- Kinematic relationship between the disk and work-piece
- Removed volume and its geometric shape

It was observed that improved model could predict cutting force during process better compared to the earlier model while it showed slight mismatch in depth of cut profile trend.

References

- [1] R. L. Kegg, "Industrial problems in grinding", *Annals of the CIRP*, Vol. 32, No. 2, pp 559-561, 1983
- [2] T. R. Kurfess, "Verification of a dynamic grinding model", *Trans. ASME, J. Dynamics, System, Measurement and Control*, Vol. 110, No. 4, pp. 403-409, 1988
- [3] S. M. Yoo and D. A. Dornfeld, "Modeling of the flexible disk grinding process: Part I - Model development", *Proceedings of 1990 ASME Winter Annual Meeting*, Dallas Texas, 1992
- [4] G. Sathyanarayanan, "Two wavelength characteristic grain model for grinding wheel", *Annals of the CIRP*, Vol. 34, No. 1, pp 299-303, 1985
- [5] S. M. Pandit and S. M. Wu, "Characterization of abrasive tools by continuous time series", *Trans. ASME, J. Eng. Ind.*, Vol. 95, No. 1, pp 821-825, 1973
- [6] W. König, "A numerical method to describe the kinematics of grinding", *Annals of the CIRP*, Vol. 31, No. 1, pp 201-204
- [7] L. Lichun, "A study of grinding force mathematical model", *Annals of the CIRP*, Vol. 29, No. 1, pp 245-249, 1980
- [8] H. Kim and K. M. Marshek, "Belt forces with grinding", *Trans. ASME, J. Eng. Ind.*, Vol. 110, No. 3, pp 201-211, 1988
- [9] K. Keuchel, "Krafte und Kraftverteilung in der kontaktzone beim bandschleifen", *Holz als Roh- und Werkstoff*, Vol. 36, No. 3, pp 102-106, 1988
- [10] D. A. Dornfeld, "Single grit simulation of the abrasive machining of wood", *Trans. ASME, J. Eng. Ind.*, Vol. 103, No. 1, pp 1-12, 1981
- [11] S. Pandit and G. Sathyanarayanan, "A model for surface grinding based on abrasive geometry and elasticity", *Trans. ASME, J. Eng. Ind.*, Vol. 104, No. 3, pp 349-357, 1982
- [12] K. Nakayama, "Elastic deflection of contact zone in grinding", *Bull. Japan Soc. of Prec. Eng.*, Vol. 5, No. 4, pp 93-98, 1971
- [13] D. E. Whitney and E. D. Tungs, "Robot Grinding and Finishing of Cast Stamping Dies", *Proceedings of the 1989 ASME WAM, S. F.*, pp. 131-151, 1989
- [14] S.M. Yoo, D.A. Dornfeld and R. Lemaster "Analysis and modeling of laser measurement system performance for wood surface", *Trans. ASME, J. Eng. Ind.*, Vol. 112, NO. 1, pp. 69-77, 1989